ARTICLE

BIOTECHNOLOGY and BIOENGINEERING

Nanomechanics Controls Neuronal Precursors Adhesion and Differentiation

Elisa Migliorini,[1,2] Jelena Ban,[3] Gianluca Grenci,[1] Laura Andolfi,[2] Alessandro Pozzato,[1] Massimo Tormen,[1] Vincent Torre,[3,4] Marco Lazzarino[1,2]

[1]CNR-IOM, Area Science Park, Trieste, Italy; telephone: +33 4 56520814; fax: +33 4 56520803; e-mail: elisam@ujf-grenoble.fr

[2]CBM S.c.r.l., Area Science Park, Basovizza, Trieste, Italy

[3]SISSA, International School for Advanced Studies, Trieste, Italy

[4]Italian Institute of Technology, SISSA Unit, Genova, Italy

ABSTRACT: The ability to control the differentiation of stem cells into specific neuronal types has a tremendous potential for the treatment of neurodegenerative diseases. In vitro neuronal differentiation can be guided by the interplay of biochemical and biophysical cues. Different strategies to increase the differentiation yield have been proposed, focusing everything on substrate topography, or, alternatively on substrate stiffness. Both strategies demonstrated an improvement of the cellular response. However it was often impossible to separate the topographical and the mechanical contributions. Here we investigate the role of the mechanical properties of nanostructured substrates, aiming at understanding the ultimate parameters which govern the stem cell differentiation. To this purpose a set of different substrates with controlled stiffness and with or without nanopatterning are used for stem cell differentiation. Our results show that the neuronal differentiation yield depends mainly on the substrate mechanical properties while the geometry plays a minor role. In particular nanostructured and flat polydimethylsiloxane (PDMS) substrates with comparable stiffness show the same neuronal yield. The improvement in the differentiation yield obtained through surface nanopatterning in the submicrometer scale could be explained as a consequence of a substrate softening effect. Finally we investigate by single cell force spectroscopy the neuronal precursor adhesion on the substrate immediately after seeding, as a possible critical step governing the neuronal differentiation efficiency. We observed that neuronal precursor adhesion depends on substrate stiffness but not on surface structure, and in particular it is higher on softer substrates. Our results suggest that cell–substrate adhesion forces and mechanical response are the key parameters to be considered for substrate design in neuronal regenerative medicine.

Biotechnol. Bioeng. 2013;110: 2301–2310.

KEYWORDS: neuronal precursor cells; neuronal differentiation; polydimethylsiloxane (PDMS); adhesion; nanotopography

Introduction

The most promising approach toward the treatment of brain neurological disorders currently involves cell therapy and tissue engineering. However, severe limitations still hinder the application of these emerging technologies at a clinical level (Delcroix et al., 2010).

Embryonic stem (ES) cells, when removed from the in vivo stem cell niche and cultured in vitro, can be forced to differentiate into neurons, using specific biochemical factors, such as growth factors and cytokines (Barberi et al., 2003), and then transplanted for the treatment of neuronal damage. However, the differentiation process is still inefficient, hard to control and usually results in a heterogeneous population with a risk of teratoma formation (Ding and Schultz, 2004; Thomson et al., 1998). For these reasons new protocols are investigated with the ambitious target of a complete neuronal differentiation.

Cells interact with the external environment not only through chemical cues but also by sensing physical properties of the environment (Curtis and Varde, 1964; Weiss and Garber, 1952). The chemistry and physics of the micro and nanoenvironment where stem cells differentiate influence and determine the phenotype, fate and functions of differentiated cells (Engler et al., 2007; Kloxin et al., 2010; McNamara et al., 2010; Tee et al., 2011).

Elisa Migliorini's present address is Fondation Nanosciences, 23 rue des Martyrs, 38000 Grenoble, France. DCM-i2bm, 570 rue de la Chimie, BP 53 38041 Grenoble Cadex 9, France.

Gianluca Grenci's present address is Mechanobiology Institute, National University of Singapore, T-Lab, #05-01 5A, Engineering Drive 1, Singapore 117411, Singapore.

Correspondence to: E. MigliориniG. Grenci

Contract grant sponsor: 7th European Framework Program

Contract grant number: 214566

Additional supporting information may be found in the online version of this article.

Received 9 September 2012; Revision received 14 January 2013;

Accepted 11 February 2013

Accepted manuscript online 22 February 2013;

Article first published online 16 March 2013 in Wiley Online Library (http://onlinelibrary.wiley.com/doi/10.1002/bit.24880/abstract)

DOI 10.1002/bit.24880

The natural environment of stem cells has a complex chemical and physical structure that differs enormously from that of the glass coverslips used in standard cell cultures. This mismatch is likely to introduce artifacts and not clearly understandable results (Franze, 2011). To improve the efficiency of the differentiation process new substrates which mimic the natural extracellular matrix (ECM) and thus emulate the actual in vivo conditions should be designed.

The effect of substrate topography has been investigated at the micrometrical and nanometrical scale (Christopherson et al., 2009; Markert et al., 2009; Park et al., 2007; Smith et al., 2009a; Wang et al., 2010; Yim et al., 2007). ES cell differentiation was induced by using the BioSurface Structures Array, that is, a microstructured surface library made of silicon lines, bars, and pillars coated with tantalum oxide with a lateral size varying from 1 to 8 μm and with 1 μm spacing (Markert et al., 2009). Nanometric gratings made of poly(L-lactic acid) matrices in the range between 50 and 500 nm, promoted ES cells spreading and differentiation (Smith et al., 2009b). Gratings of sub-micrometric periods exhibited an effect also on mesenchymal stem cells (MSCs). Lines 350 nm wide, made of polydimethylsiloxane (PDMS), increased neuronal differentiation with respect to flat controls (Yim et al., 2007). Polyethersulfone fiber mesh, 700 nm in diameter, increased rat neuronal precursors differentiation (Christopherson et al., 2009).

The protein arrangement on a flat substrate has also been tested to control neuronal differentiation. Neuronal precursors grown on a microarray of proteins (Soen et al., 2006) showed that a combination of Wnt3a and laminin had a neurogenic effect.

Several groups demonstrated that cell fate can be manipulated by the mechanical properties of the substrates (Discher et al., 2005; Engler et al., 2006; Wang et al., 2012). Brain ECM mechanical properties were well characterized and it was demonstrated that soft substrates in the range between 100 Pa and 1 kPa directed the formation of neurite branches, critical for synaptic connections during development (Flanagan et al., 2002) and enhanced MSC and neuronal precursor differentiation into neuronal lineage (Engler et al., 2006; Leipzig and Shoichet, 2009). Both topographic and mechanical properties of the contact surface are processed by mechanotransductive pathways that include the activation of focal adhesion proteins, such as vinculin, paxilin, talin, and cytoskeletal networks which generate an alteration of the cellular properties (Bershadsky et al., 2006; Tee et al., 2011). Mechanical stress leads to the activation of transcription factors that can translocate to the nucleus and modify gene expression (Alenghat and Ingber, 2002). In spite of the importance of stem cell adhesion on their differentiation, no quantitative physical measurements of the adhesion forces have been reported yet.

Mechanical and geometrical cues are often considered separately, although a significant interplay correlates these two major aspects: for instance resizing a material will intrinsically affect its mechanical properties, and, conversely, very soft materials can be obtained only in structured materials with a well-defined 3D nanogeometry or nanoporosity, or with different chemical composition. A definitive experiment able to provide to each factor the correct weight is still missing.

In a previous work we observed that growing neuronal precursors on polydimethylsiloxane (PDMS) substrates nanopatterned with arrays of pillars, coated with laminin, enhances the neuronal differentiation, with a major improvement in the early stage of the differentiation process (Migliorini et al., 2011). However we did not consider the mechanical properties of the substrates, and in particular we were not able to separate the stiffness effect from the topographic effect. In this manuscript we report on new experiments aimed at understanding the role of the mechanical properties of nanostructured substrates. We fabricated a new set of substrates with comparable effective stiffness but different topography and same topography with different effective stiffness. For each substrate we evaluated the differentiation yield and, using single cell force spectroscopy (SCFS), we measured the adhesion of neuronal precursors immediately after plating. Cross correlating the experimental data allowed us to establish which parameter is more relevant to control the differentiation efficiency.

Materials and Methods

Fabrication of Nanopatterned Substrates

Nanopatterned substrates were fabricated according to a previously established method (Migliorini et al., 2011).

Master Fabrication

Commercial gratings of lines (250 nm width and 500 nm period) produced by interference lithography (IL) and etched into silicon to a depth of 320 nm were purchased from Amo GmbH (Achen, DE). Silicon moulds with depth of 50–400 nm were obtained from the primary gratings by single step or double step nanoimprint lithography (NIL) process followed by plasma etching as reported in the supplementary information 1.

Fabrication of Soft PDMS Substrates

Substrates for cell culture were obtained by mold casting as reported in the supplementary information 1. To avoid the collapse of PDMS nanostructures, due to capillary forces in the liquid, it was permanently made hydrophilic using a 2-hydroxyethyl methacrylate (HEMA) (Sigma-Aldrich CHEMIE GmbH, Taufkirchen, Germany) coating reproducing a process reported in (Bodas and Khan-Malek, 2007). Flat and softer PDMS was obtained by mixing the curing

agent at 2% (w) to the base followed by degassing under vacuum for 30 min and curing at 60° overnight (18–20 h).

Fabrication of Hard Glass-Like Substrates

Hard, glass-like nanostructured substrates were fabricated as reported in Figure 1. Three hundred fifty nanometers thick Hydrogen Sylses Quioxane (HSQ) based resist (mr-I 7000E, Dow Cornig Corp., Midland, MI) was spin coated on top of circular glass cover slides (24 mm diameter). The residual solvent in the film was removed by annealing on a hot plate at 200°C for 15 min. A silicon master with pillars of 220 nm × 220 nm base, 250 nm height and 500 nm period was used to perform a NIL process on a film of mr-7010a resist (Micro Resist Technology, GmbH, Berlin, Germany), spin coated on the HSQ-coated glass cover slide. After the removal of the residual layer by oxygen plasma, the pattern resulting from the NIL process was transferred by lift-off of 10 nm of chromium, which was subsequently used as etching mask in a fluorine-based plasma etching process in an ICP reactor (SPTS Technologies, Newport, UK), resulting in extended arrays of pillars in the HSQ layer. A final height of 360 nm was achieved after 10 min of etching process, that is, at an etching rate of 0.6 nm/s. After the etching, the Cr was removed in a wet etching bath (35 mL acetic acid in 600 mL water and 200 g of ammonium cerium nitrate salt); finally, the HSQ structure was converted to a silicon oxide by an overnight thermal treatment at 400°C in air.

Substrate Characterization

Atomic force microscopy (AFM) of HEMA hydrophilized nanopatterned substrate was performed using a Nanowizard II AFM (JPK Instrument, Berlin, Germany) combined with an inverted optical microscope (Zeiss Axiovert 200, Göttingen, Germany). The effective elastic modulus of substrates was measured by AFM force spectroscopy as reported in the supplementary information 2.

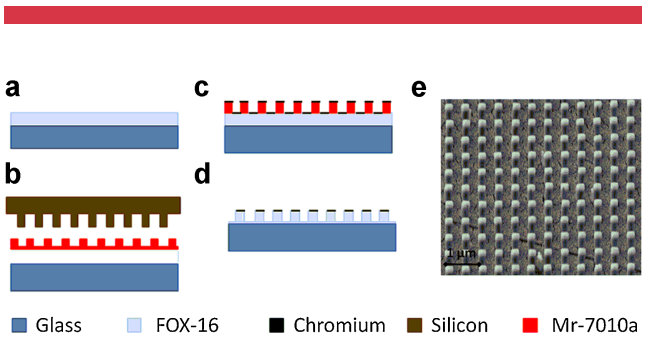

Figure 1. Fabrication of nanopatterned glass substrates. **a**: HSQ (FOX-16) spin coating; (**b**) Si master NIL on Mr-7010a coated on the top of glass + HSQ; (**c**) Cr sputtering; (**d**) etching in a fluorine-based ICP reactor; (**e**) SEM images of glass pillars obtained (scale bar 1 μm).

Embryonic Stem Cells Culture and Stromal Cell-Derived Inducing Activity (SDIA) Protocol

ES cells were induced to differentiate into neurons as previously described (Ban et al., 2007) and as reported in the Supplementary Information 3.

Immunocytochemistry

The whole information regarding the immunocytochemistry assays on cells and on substrates are reported in the Supplementary Information 4.

Statistical Analysis

The percentage of neuronal precursors differentiation, cells survival, neuritis length, and cellular adhesion forces, are presented as mean values ± standard deviation. All data were collected from at least three independent experiments.

To evaluate statistical significance between the mean values of couples of samples an unpaired Student's *t*-test was applied and a *P*-value was extracted. For of more than two samples the ANOVA test was applied using the Bonferroni correction. A *P*-value with $\alpha = 0.05$ was extracted for each samples combination.

AFM setup and Single Cell Force Spectroscopy (SCFS) Analysis

SCFS was performed using a Nanowizard II AFM (JPK Instrument) equipped with a CellHesion module (JPK Instrument) that extended the vertical range up to 100 μm by piezo-driven movements of the sample holder. Tipless silicon nitride V-shaped cantilevers, 200 μm in length, having a nominal spring constant of 0.06 N/m (VEECO NP-010) were cleaned with a H_2SO_4 solution and activated with O_2 plasma treatment for 3 min at a pressure of 100 μbar, flow rate 20 sccm and an RF power of 100 W for 3 min. SCFS analysis cantilever were functionalized with fibronectin 10 μg/mL and stored in PBS 1% at 4°C one day before each experimental run. Cantilever spring constant and optical levers were individually calibrated in liquid on a rigid glass surface.

Neuronal precursors were mechanically dissociated from the substrate and from each other and incubated 15 min in HBSS solution. Isolated cells were pipetted into the AFM sample chamber and captured over a 1% BSA-coated area. A single cell was pressed on the BSA-coated surface with a contact force of 200 pN for 30 s. The cell was lifted from the surface and allowed to form a firm adhesion with the cantilever.

The cell was pressed on the substrate functionalized with laminin with 500 pN contact force, and then maintained in contact for a pre-defined time in the range from 20 s to 5 min. The force was kept constant by the AFM closed loop feedback. After contact time the cell was withdrawn at a

constant speed of 5 μm/s for 50–70 μm and the cantilever deflection, that is, the adhesion force versus distance is recorded. Bonds between cell and substrate break sequentially, causing sudden changes in the cantilever deflection, until cell, and substrate are completely separated.

To compare the adhesion of neuronal precursors on different substrates during different contact times the same cell was used to acquire three force–distance curves for each contact time and for each substrate in a random sequence. The longest contact times (>160 s) were left at the end of the experiment because of the high risk of cell detachment.

After each force measurement, the cells was retracted to recover for a period of time greater than the contact time with the surface before adhering to a different spot on the surface.

For SCFS analysis around 30 force distance curves for each contact time and for each substrate were acquired and analyzed with JPK Image processing (Berlin, Germany) and data represented into graphics using IGOR Pro 5 (WaveMatrics, Portland, OR) and Origin 8.1 (Origin Lab Corporation, Northampton, MA).

Results

We previously demonstrated (Migliorini et al., 2011) that neuronal precursors differentiation into neuronal lineage was enhanced when the substrate was patterned with nanometric structures. Indeed, 96 h after plating on PDMS, neuronal precursors exhibited a neuronal yield of ~60% on flat substrates and of ~80% on nanostructures with aspect ratio as high as 1.44 (360 nm high, 250 wide, and 500 nm period nanopillars). In that particular set of experiments pillars were made with PDMS. The largest relative difference in terms of neuronal yield on nanopatterned versus flat substrates was obtained at 6 h after plating, suggesting the presence of a mechanism that accelerates the differentiation, probably related to the different cell–substrate interaction after precursor plating.

Effect of the Nanopattern on Neuronal Differentiation

The first question we aimed at answering with this manuscript is whether the substrate geometry alone is able to increase the differentiation yield. To this purpose, we fabricated hard glass substrates with the same nanostructures described above. The effect of soft and hard nanopillars on neuronal differentiation was evaluated and compared to that of PDMS and glass flat substrates and commercial glass coverslip controls. ES-derived neuronal cultures were fixed after 48 h and immunostained for Tuj1 (antibody against neuronal class III β-tubulin), nestin (neuronal precursors marker), and Hoechst (nuclei staining) (see the Fabrication of Hard Glass-Like Substrates Section). Figure 2a–d shows representative fluorescence images of ES-derived neural cultures on soft and hard pillars, on flat PDMS and on glass. We first analyzed the precursor survival after 48 h, observing no significant differences between all the five substrates. Survival data are reported in the supplementary information (Table S1). The observed neuronal yield is reported in Figure 2e. All the substrates under investigation provided comparable differentiation yield, with exception of PDMS pillars that showed an increase of about 20%. The effect of PDMS nanopillars is statistically significant: unpaired Student's *t*-test provided a *P*-value between 0.003 and 0.007 between PDMS nanopillars and the other substrates (Fig. 2e). Therefore, both imposing a nanostructure on hard substrates and changing the stiffness of flat substrates did not induce any increase of the differentiation yield, and only the combination of nanopattern and material provides an effect on the differentiation yield. We could thus exclude that the effect observed in our previous paper was generated by an easier access to the growth medium, obtained suspending the neuronal precursors over the pillar "bed." We also verified whether the particular structure of PDMS pillars presented a larger concentration or a different distribution of the laminin coating used to improve cellular adhesion. Fluorescent images of flat and patterned substrates (see Fig. S1) show clearly that laminin is uniformly distributed in both substrates with an equivalent density of laminin-fluorophore clusters. The integrated fluorescence is slightly larger on the flat substrates, which can be explained by the reduced surface available in the case of the patterned substrate.

Neuronal Differentiation on PDMS Nanopillars with Different Mechanical Properties

The second question we aimed to answer with this paper is whether the different substrate mechanical properties, namely substrate stiffness, are the cause of the different differentiation yield. To this purpose, we analyzed by AFM force spectroscopy the mechanical properties of the nanopatterned PDMS substrates. Squared pillars 250 nm width and increasing height (35, 100, and 360 nm) were analyzed. As reported on paragraph 2.2 we used a tipless cantilever on which we glued a 5 μm diameter glass bead (Fig. 3a). We choose to use beads with a diameter larger that the substrate periodicity to measure the effective elastic response of the substrate and not the response of individual pillars. The latter depend on how and where the force is exerted and can be dominated by bending, compression or shearing with different mechanical constants. Therefore the actual elastic constant could differ significantly from the one derived from the pillar bending (Schoen et al., 2010). The response to a large bead is, on the contrary, a combination of all those effects effect and it does not depend on the exact location where the force is exerted. For small displacements this response is linear with the force and it is possible to introduce an effective compressibility value of the substrate measured with a bead which we will denote as E_B which depends on the bead size and should not be intended as a

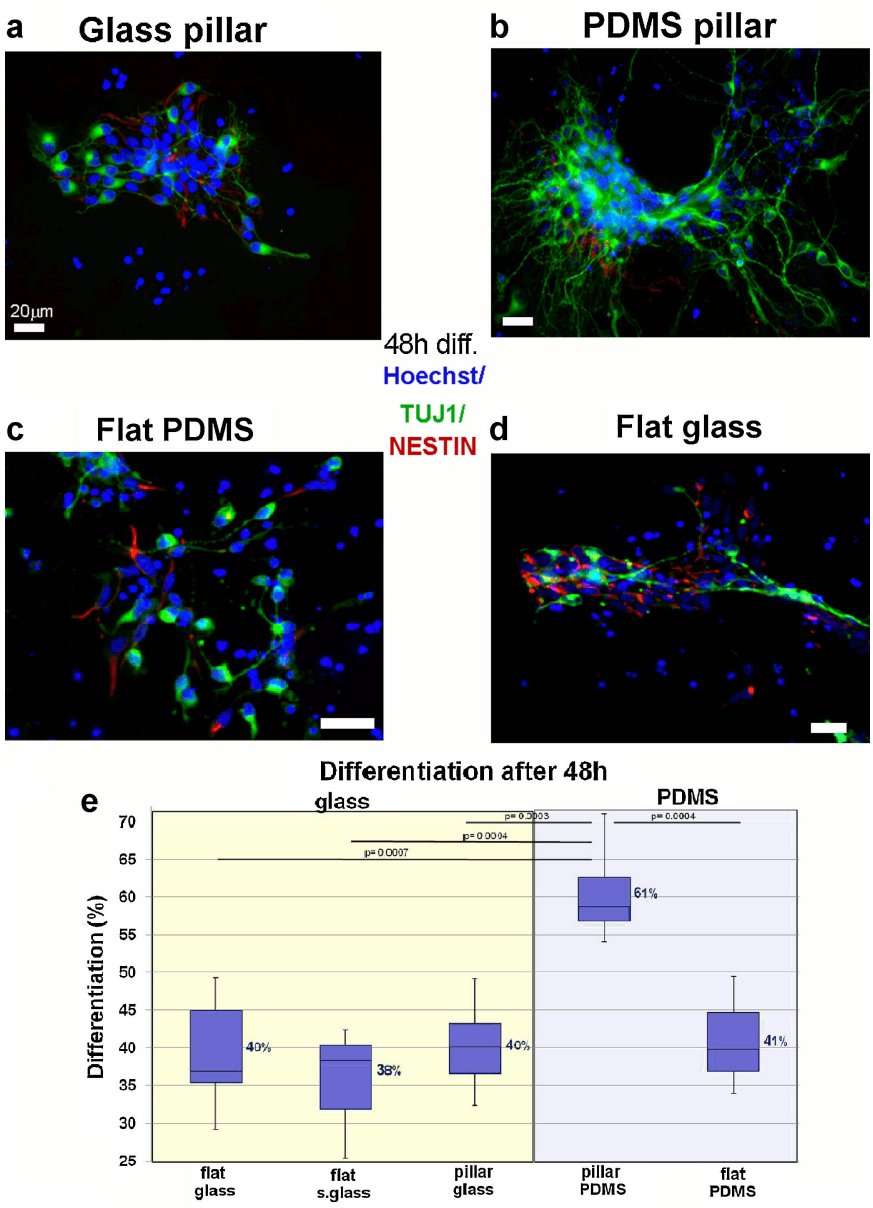

Figure 2. Neuronal precursors differentiation induction on rigid glass-like and on soft PDMS pillars. **a** and **b**: IF representative images of ES derived cell culture on glass-like pillars (a) on PDMS pillars (b) on flat PDMS with E_B of 456 kPa (**c**) and on flat glass (**d**); neurons were labeled with Tuj1 (green), neuronal precursors with nestin (red) and nuclei were stained with Hoechst. (**e**) Box plot which represents the distribution of the neuronal differentiation on flat controls (PDMS, glass and standard glass substrates) and on nanopatterned substrates (glass and PDMS nanopillars). The values inside the boxes represented the range between the first and the third quartile (the half of the values) and the line in the box is the median. The mean value of differentiation was written as percentage in the right of each box. Numbers between bars indicate the *P*-value of Student's *t*-tests.

material properties. We chose a bead size comparable to that of a neuronal precursor before plating, so that the measured stiffness can be interpreted as the effective stiffness experienced by the cell when plated.

Representative force–distance curves for each substrate are reported in Figure 3b. The average E_B is plotted versus pillars height (Fig. 3c) and ranges between 40 kPa (360 nm height pillars) to 300 kPa (50 nm height pillars). Therefore it is possible to significantly change the substrate elasticity increasing pillars aspect ratio, indeed the differences between substrates E_B are always significant with *P*-values smaller than 0.001. The large distribution of the E_B values can be ascribed more probably to the method used to evaluate the substrate rigidity, which considers only the average compressibility of the pillars but not the local interaction of the cell with single pillars.

Neuronal differentiation was evaluated 48 h after neuronal precursors plating. We observed a clear correlation

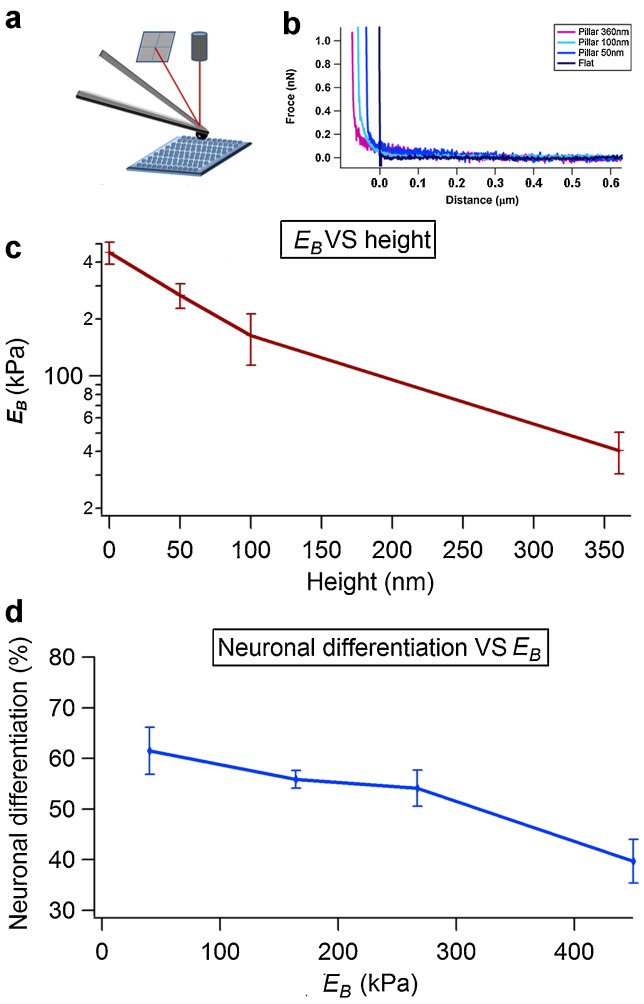

Figure 3. Mechanical characterization of the nanopatterned substrates using AFM force spectroscopy. **a**: Representation of an AFM cantilever with a bead attached to the end. **b**: Examples of force–distance curves acquired; **c**: pillars compressibility value E_B plotted versus pillars heights. **d**: Neuronal differentiation plotted versus substrates E_B.

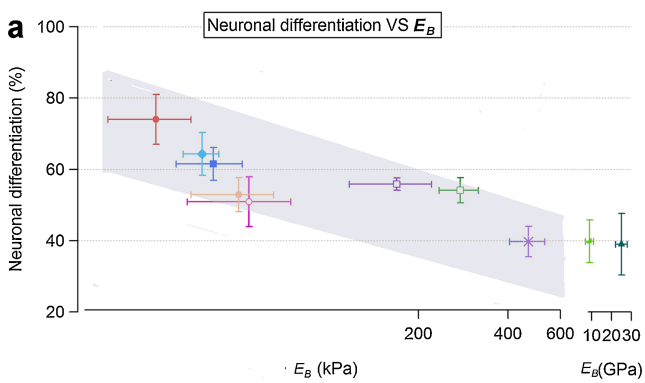

b

Symbols	Pitch (nm)	Height (nm)	Wide (nm)	E_B (Kpa)	Neuronal diff. (%)
●	500	340	150	26 ± 7	74 ± 7
■	500	360	250	40 ± 10	61 ± 4
●	500	160	200	49 ± 7	53 ± 5
○	500	100	150	53 ± 5	51 ± 7
□	500	100	250	164 ± 40	56 ± 2
□	500	35	250	267 ± 50	54 ± 3
◆	Flat 2%	-	-	38 ± 13	64 ± 6
✱	Flat 10%	-	-	456 ± 60	40 ± 8
▲	Flat glass	-	-	$2.6 \cdot 10^6 \pm 3 \cdot 10^5$	39 ± 8
◢	Glass pillar	360	250	$8.9 \cdot 10^5 \pm 20 \cdot 10^4$	39 ± 9

Figure 4. Neuronal differentiation versus E_B. **a**: Semi-log plot of neuronal differentiation versus substrate E_B. Symbols are related to different types of substrate. The gray band is an eye guide to highlight the increased differentiation as a function of the E_B. **b**: List of substrates geometrical and mechanical characteristics with the corresponding value of neuronal differentiation and symbols used in the previous graph.

between substrate rigidity and differentiation yield, with the latter increasing on softer substrates (Fig. 3d). In order to evaluate the statistical significance of the differentiation enhancement on nanostructured substrates versus flat surfaces we applied the ANOVA test. Details are provided as supplementary information (Table S2). In summary 40 kPa nanostructured substrates (250 nm wide and 360 nm height) provides a significant increase of differentiation yield (+20% *P*-value 0.004) with respect to the flat PDMS with an E_B of 456 kPa, while 180 and 300 kPa show a large but statistically poor increase of neuronal differentiation (+15% *P*-value 0.14 and +12%, *P*-value 0.22 respectively). To further decrease E_B without changing the substrate chemistry and maintaining the same periodicity we fabricated thinner nanopillars of 150 nm width, 100 nm and 340 nm height and pillars of 200 nm width and 160 nm height. In this way the E_B measured for the highest pillars was 26 ± 7 kPa (Fig. 4a red dot). We evaluated neuronal differentiation on these pillars after 48 h with Tuj1 and Hoechst immunostaining: Figure 4b summarizes all the data and highlights a clear dependence of neuronal differentiation on the substrate elasticity.

Neuronal differentiation increased with decreasing of the E_B also on the set of pillars with 150 nm width. On the tallest pillars of this set, with $E_B = 26$ kPa, the neuronal differentiation after 48 h increased significantly up to 74 ± 7% (Fig. 4b red dots and Table S2). Neuronal yield was not significantly different for substrates of different geometry but similar elasticity, as for instance for 150 nm, 100 nm height pillars (pink hollow dot) and 200 nm width and 160 nm height pillars (Fig. 4b orange hollow dot) (*P*-value = 1).

E_B was changed on flat PDMS substrates by decreasing the percentage of cross-linker from 10% to 2% (Brown et al., 2005). In this way the E_B decreased from 456 kPa (Fig. 4b violet asterisk) to less than 38 kPa (Fig. 4b, sky-blue diamond). Interestingly, neuronal differentiation on the soft but flat PDMS was very similar to the differentiation

on nanopillars with an equivalent value of E_B (Fig. 4b, blue box): $64 \pm 6\%$ and $61 \pm 1\%$, respectively (P-value $= 1$).

In the same way, for the substrates with E_B larger than 400 kPa (flat 10%, flat glass, glass pillars), neuronal yield never exceeded 40% independent of material used, chemistry and surface geometry. Indeed the statistical comparison between the mean values shows a not significant differences between these substrates with P-values >0.4 (see Table S2).

Summarizing, neuronal differentiation increases for substrate E_B less than 400 kPa. On the other hand, in our experiment the substrate geometry does not play any role but further tuning the substrate mechanical properties. To better understand how the pillar nanostructures mediate the cell–substrate interaction, neuronal precursors were plated on the softer substrate used (26 kPa see Fig. 4b), fixed in PFA after 2.5 h, dehydrated in water:ethanol mixtures at increasing ethanol content (50:50; 20:80; 10:90; pure ethanol), gold-sputtered and imaged with a scanning electron microscope (SEM). A representative SEM image is provided as supplementary information (Fig. S2). We observed that cells exert a strong pulling forces on the substrates, and the lateral compliance of the pillar structure clearly accommodate cell morphology.

The effect of the substrate on cellular morphology was analyzed comparing neurites length on five different substrates: pillar 40 kPa, glass pillar, pillar 26 kPa, flat PDMS 38 kPa and flat PDMS 456 kPa (Fig. 5a and b). As shown in Figure 5b, the neurites length is inversely proportional to the substrate stiffness, with average length of 42 μm on the softer substrate and only 22 μm for the glass substrate. The average lengths for substrates with different stiffness are all statistically independent, with the exception of the pillar at 40 kPa and the flat PDMS with 2% of cross linker, which have comparable stiffness and undistinguishable neurite average length (see Supplementary Information Table S3 for details).

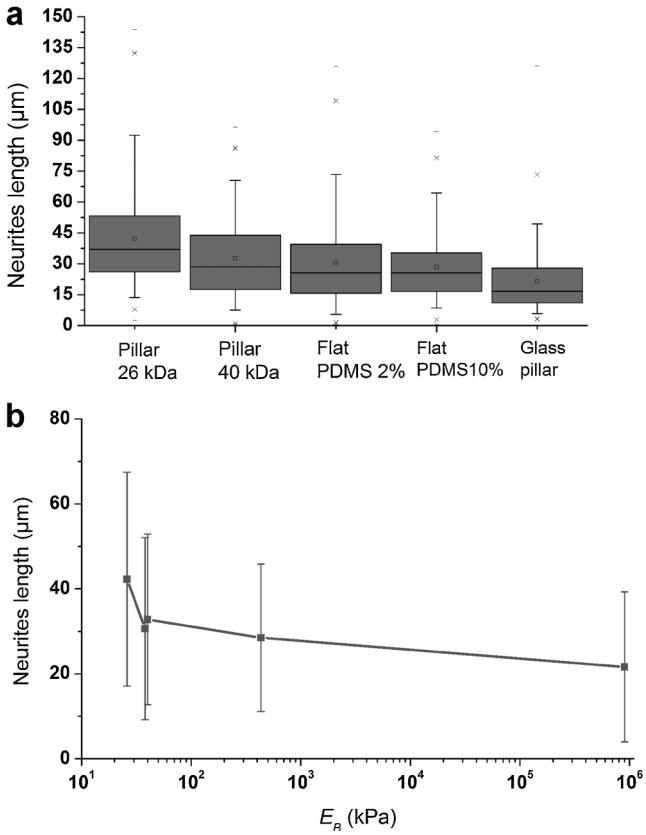

Figure 5. Neurites length versus E_B. **a**: The boxplot represents the distribution of neurites length on five different substrates indicated in the *x*-axis. The values inside the boxes represented the range between the first and the third quartile (the half of the values) and the line in the box is the median. The mean value is represented by an empty square inside the box, the minimum and the maximum value by a minus (−) and the 99th value by an asterisk (*). **b**: Semi-log plot of neurites length over substrates E_B.

Adhesion of Neuronal Precursors on PDMS Nanopillar

The last question we aimed at answering is about the reason for which a softer substrate gives a higher differentiation yield. The main role of a substrate during the differentiation process is to provide a suitable support for adhesion and growth (Engler et al., 2006; Geiger, 2001; McBeath et al., 2004; Zajac and Discher, 2008). Therefore, we focused our attention on the cell–substrate adhesion, and in particular on the early adhesion stage after plating, as the substrate seems to play a role mainly in the first 6 h (Migliorini et al., 2011). To investigate the mechanical interaction between neuronal precursors and substrates during precursors plating, we performed SCFS.

We investigated the precursors adhesion on PDMS nanopillars, on flat PDMS with two different compositions (456 and 23 kPa respectively) and on glass nanopillars, during the first minutes of cell–substrate interaction. The range of contact time considered was between 20 s to 5 min. From the resulting force–distance curves (a typical curve is shown in Fig. 6a) the maximal detachment force (F_{detach}), needed to remove the cell from the substrate, was determined from the cantilever deflection during retraction. F_{detach} was averaged from almost 30 events recorded for each substrate and is plotted (Fig. 6b) versus the substrates' E_B.

We found that the force needed to detach a neuronal precursor from the PDMS nanopillars was significantly higher than the F_{detach} on flat PDMS and on glass nanopillars, indeed already after 20 s of adhesion time the differences between the substrates are significant (P-value <0.01). We ruled out the hypothesis that the different adhesion was determined by a different laminin concentration or arrangement on the different surfaces, since, as previously discussed and shown in supplementary Figure S1, we did not observe a significant difference in laminin coatings.

Similar measurements on flat and patterned PDMS were performed plating fibroblasts as a control condition, and no

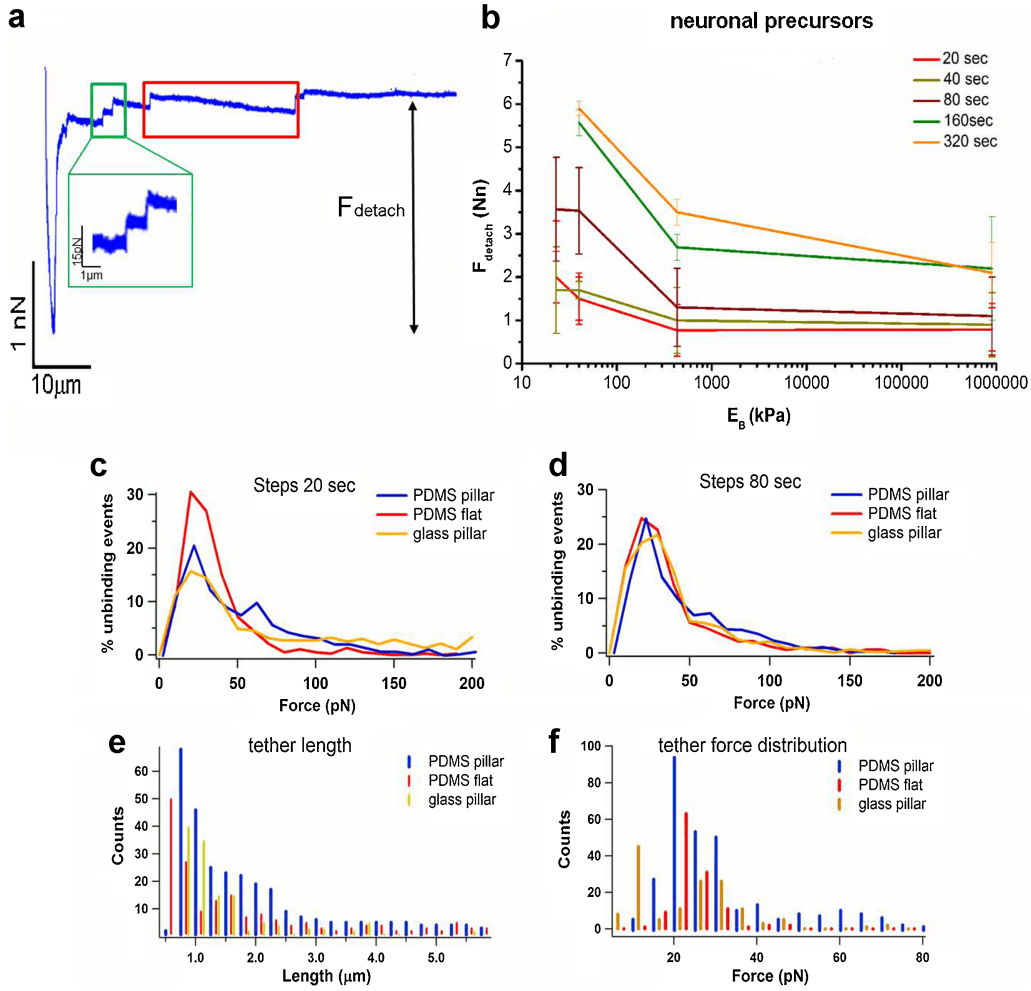

Figure 6. SCFS analysis on glass pillars, flat PDMS and PDMS pillars. **a**: Representative example of force–distance curves acquired on PDMS nanopillars where is indicated by an arrow the force necessary to detach the cells from the substrate, by a red square a tether pulled out from the cellular membrane and by a green square the "steps" which are single unbinding events corresponding to ruptures between cellular membrane and the substrate. **b**: Graphs of the maximum adhesion force of neuronal precursors on substrates with different E_B. The different colored lines correspond to different contact times between the cell and the substrate. **c**: Single unbinding event analysis after 20 s. **d**: After 80 s of contact time on the three different substrates (PDMS pillar, flat PDMS 456 kPa and glass pillars). **e**: Tether length distribution on the three substrates previously reported; **(f)** distribution of the forces needed to pull a tether out of the membrane.

differences in terms of adhesion between patterned and non patterned PDMS were observed (Fig. S3). The increased adhesion on PDMS nanopillars was specific for neuronal precursors. As shown in the force–distance curve (Fig. 6a) we were able to pull tethers out of neuronal precursor membranes. Indeed several plateaus of a length in the range between 1 and 15 µm were obtained after 40 s of adhesion time. Each plateau corresponds to a single tether and the height of the step can be associated to the force needed to pull a single tether out of the membrane (Sun et al., 2005).

The forces needed to pull the tether were comparable and between 15 and 40 pN for PDMS nanopillar, flat PDMS (456 kPa) and glass pillar. Also the length of tethers was similar in the three different substrates, while the tether number was larger for cells interacting with PDMS nanostructured substrates. Single step analysis at different adhesion times reported in Figure 6c showed a peak around 30 pN for all substrates. On PDMS pillars we observed also a small peak at 60 pN that could originated from multiple cellular receptor-ECM ligand unbinding events. The formation of multiple adhesion points could explain the stronger average adhesion of neuronal precursors on nanopillars.

Discussion

In this manuscript we investigated the geometrical and the mechanical contributions of sub-micrometric PDMS pillars to the differentiation of ES-derived precursors into neuronal lineage. This analysis was never addressed in literature so far, indeed the effect of the nanopattern and of the elasticity of

the substrates were always evaluated separately (Dalby et al., 2002; Dulgar-Tulloch et al., 2009; Engler et al., 2006; Ferrari et al., 2010) even if they are intrinsically correlated. We observed that the reduction of the substrate stiffness alone can promote a neuronal differentiation enhancements. The stiffness modulation can be obtained either by varying the chemical composition of the elastomeric substrate or by introducing nanostructures with increasing aspect ratio. We proved that the nanostructure alone has no effect on differentiation by comparing flat rigid substrates, nanostructured rigid substrates and nanostructured soft substrates. Only in the latter case the differentiation yield was affected.

We hypothesize that the improvement in differentiation yield was a consequence of a stronger and faster adhesion of neuronal precursors on the differentiation substrates. Indeed, performing SCFS measurements, we observed that adhesion forces increased up to a factor three on softer substrates, regardless of the geometric parameters. The single step analysis showed that, on PDMS nanopillars, the number of single focal adhesions is larger than on flat PDMS (456 kPa) and glass nanopillars, that is in agreement with the overall stronger adhesion on the PDMS nanopillars. The tether analysis was not performed on the softest substrate (flat PDMS with E_B of 23 kPa), since it was not possible to neglect the substrate compliance contribution. Examples of ideal force–distance curves, where tethers can be analyzed, and compliant–substrate curves were shown in the Supplementary Information (Fig. S4). The forces applied for tethers ruptures were comparable for the three substrates, indeed these forces depend only on the cell membrane effective surface viscosity and on its association with the underlying cytoskeleton (Sun et al., 2005) and not on the substrate structure. All these results indicated a major importance of substrate rigidity rather than substrate geometry.

The mechanism at the base of the increased/faster adhesion of neuronal precursors might involves the activation of the integrin-mediated focal adhesion complexes pathways (Burridge et al., 1988). Indeed focal adhesions play an important role in the linking of the actin filaments to the transmembrane integrins (Geiger, 2001).

A preliminary Paxillin staining of neuronal precursors after 2.5 h plating on nanostructured and flat PDMS substrates is reported in Figure S5. In both cases Paxillin is expressed with comparable level. However no significant spatial re-arrangement can be observed on the nanostructured substrates, within the spatial resolution of the microscope used. Further investigation should be performed with super-resolution techniques. The clear correlation between enhanced differentiation yield and a faster and more efficient adhesion on the same kind of substrate suggests that the mechanical enhancement of neuronal differentiation is triggered by the increased adhesion on softer substrates. Geometrically different pillars with the same E_B gave the same neuronal yield, moreover neuronal differentiation on flat PDMS substrates with 2% of cross-linker was comparable to the one obtained with PDMS nanopillars 360 nm height and 250 nm width which had similar elastic properties. Therefore the neuronal differentiation was modulated changing the substrates mechanical properties independent of the geometrical ones. The substrate elasticity can be tailored by fabricating different PDMS nanostructures using the recommended percentage (10%) of cross-linker (Taylor et al., 2003), as we did for the fabrication of nanopillars, or by reducing the percentage of cross-linker down to 2%, with flat topography. However, the reduction of cross-linker results in residual monomers, which are mobile and free to migrate to the surface of the substrate and contaminate the culture (Lee et al., 2003). It was demonstrated indeed that different compositions of PDMS may affect cell behavior (Lee et al., 2004). In particular it was shown that fibroblasts do not grow and die when the cross-linker percentage is below 5% (Mirzadeh et al., 2003). In our experiments with 2% concentration of cross-linker we did not observe a significant alteration on cellular growth but an increased cellular adhesion with respect to the standard PDMS (Fig. 6b). However our data were limited to 48 h after plating, while the monomer effect was observed for longer times. For this reason using a purely chemical approach in the context of regenerative medicine might be risky, since long-term chemical effects might be difficult to predict. Our results demonstrated that by surface nanostructuring it is rather easy to control the mechanical properties of the substrate, and this control of mechanical properties can be exploited to enhance neuronal precursor differentiation, avoiding the introduction of less controllable chemical variables.

Finally, we believe that our results should be interpreted within the general framework of stem cell "mechano-niche," where it is the specific combination of cell mechanical properties, ECM stiffness and external mechanical cues that drives the maintenance and the development of stem cell population (Lee et al., 2011).

Conclusions

In this manuscript the contribution of nanoscale topography and of the elasticity of the substrate on neuronal differentiation were compared. We demonstrated that the elasticity of the substrates has a key role on the induction of neuronal precursors differentiation. We showed that lowering the substrate stiffness results in a significantly stronger neuronal precursors–substrates adhesion, which in turn could properly guide the differentiation process. The highest neuronal yield was obtained on pillars with an E_B of 26 kPa. Being able to further decrease the substrate E closer to the in vivo values coupling chemical and geometrical strategies would potentially allow us to reach neuronal differentiation at higher yields.

We are grateful to Paul Jamney for critical reading of the manuscript. The research leading to these results has received funding from the

European Union's Seventh Framework Programme FP7/2007–2013 under grant agreement n. 270483 (Acronym:FOCUS).

References

Alenghat FJ, Ingber DE. 2002. Mechanotransduction: All signals point to cytoskeleton, matrix, and integrins. Sci STKE 2002 (119): e6.

Ban J, Bonifazi P, Pinato G, Broccard FD, Studer L, Torre V, Ruaro ME. 2007. Embryonic stem cell-derived neurons form functional networks in vitro. Stem Cells 25:738–749.

Barberi T, Klivenyi P, Calingasan NY, Lee H, Kawamata H, Loonam K, Perrier AL, Bruses J, Rubio ME, Topf N, Tabar V, Harrison NL, Beal MF, Moore MAS, Studer L. 2003. Neural subtype specification of fertilization and nuclear transfer embryonic stem cells and application in Parkinsonian mice. Nat Biotechnol 21:1200–1207.

Bershadsky A, Kozlov M, Geiger B. 2006. Adhesion-mediated mechanosensitivity: A time to experiment, and a time to theorize. Curr Opin Cell Biol 18:472–481.

Bodas DS, Khan-Malek C. 2007. Fabrication of long-term hydrophilic surfaces of poly(dimethyl siloxane) using 2-hydroxy ethyl methacrylate. Sens Actuators B Chem 120:719–723.

Brown XQ, Ookawa K, Wong JY. 2005. Evaluation of polydimethylsiloxane scaffolds with physiologically-relevant elastic moduli: Interplay of substrate mechanics and surface chemistry effects on vascular smooth muscle cell response. Biomaterials 26:3123–3129.

Burridge K, Fath K, Kelly T, Nuckolls G, Turner C. 1988. Focal adhesions: Transmembrane junctions between the extracellular matrix and the cytoskeleton. Annu Rev Cell Biol 4:487–525.

Christopherson GT, Song H, Mao H-Q. 2009. The influence of fiber diameter of electrospun substrates on neural stem cell differentiation and proliferation. Biomaterials 30:556–564.

Curtis AS, Varde M. 1964. Control of cell behaviour: Topological factors. J Natl Cancer Inst 33:15–26.

Dalby MJ, Yarwood SJ, Riehle MO, Johnstone HJH, Affrossman S, Curtis ASG. 2002. Increasing fibroblast response to materials using nanotopography: Morphological and genetic measurements of cell response to 13-nm-high polymer demixed islands. Exp Cell Res 276:1–9.

Delcroix GJ-R, Schiller PC, Benoit J-P, Montero-Menei CN. 2010. Adult cell therapy for brain neuronal damages and the role of tissue engineering. Biomaterials 31:2105–2120.

Ding S, Schultz PG. 2004. A role for chemistry in stem cell biology. Nat Biotechnol 22:833–840.

Discher DE, Janmey P, Wang Y-L. 2005. Tissue cells feel and respond to the stiffness of their substrate. Science 310:1139–1143.

Dulgar-Tulloch AJ, Bizios R, Siegel RW. 2009. Human mesenchymal stem cell adhesion and proliferation in response to ceramic chemistry and nanoscale topography. J Biomed Mater Res A 90:586–594.

Engler AJ, Sen S, Sweeney HL, Discher DE. 2006. Matrix elasticity directs stem cell lineage specification. Cell 126:677–689.

Engler AJ, Sweeney HL, Discher DE, Schwarzbauer JE. 2007. Extracellular matrix elasticity directs stem cell differentiation. J Musculoskelet Neuronal Interact 7:335.

Ferrari A, Cecchini M, Serresi M, Faraci P, Pisignano D, Beltram F. 2010. Neuronal polarity selection by topography-induced focal adhesion control. Biomaterials 31:4682–4694.

Flanagan LA, Ju Y-E, Marg B, Osterfield M, Janmey PA. 2002. Neurite branching on deformable substrates. Neuroreport 13:2411–2415.

Franze K. 2011. Atomic force microscopy and its contribution to understanding the development of the nervous system. Curr Opin Genet Dev 21:530–537.

Geiger B. 2001. Cell biology. Encounters in space. Science 294:1661–1663.

Kloxin AM, Benton JA, Anseth KS. 2010. In situ elasticity modulation with dynamic substrates to direct cell phenotype. Biomaterials 31:1–8.

Lee JN, Park C, Whitesides GM. 2003. Solvent compatibility of poly(dimethylsiloxane)-based microfluidic devices. Anal Chem 75:6544–6554.

Lee JN, Jiang X, Ryan D, Whitesides GM. 2004. Compatibility of mammalian cells on surfaces of poly(dimethylsiloxane). Langmuir 20: 11684–11691.

Lee DA, Knight MM, Campbell JJ, Bader DL. 2011. Stem cell mechanobiology. J Cell Biochem 112:1–9.

Leipzig ND, Shoichet MS. 2009. The effect of substrate stiffness on adult neural stem cell behavior. Biomaterials 30:6867–6878.

Markert LD, Lovmand J, Foss M, Lauridsen RH, Lovmand M, Füchtbauer E-M, Füchtbauer A, Wertz K, Besenbacher F, Pedersen FS, Duch M. 2009. Identification of distinct topographical surface microstructures favoring either undifferentiated expansion or differentiation of murine embryonic stem cells. Stem Cells Dev 18:1331–1342.

McBeath R, Pirone DM, Nelson CM, Bhadriraju K, Chen CS. 2004. Cell shape, cytoskeletal tension, and RhoA regulate stem cell lineage commitment. Dev Cell 6:483–495.

McNamara LE, McMurray RJ, Biggs MJP, Kantawong F, Oreffo ROC, Dalby MJ. 2010. Nanotopographical control of stem cell differentiation. J Tissue Eng 2010:120623.

Migliorini E, Grenci G, Ban J, Pozzato A, Tormen M, Lazzarino M, Torre V, Ruaro ME. 2011. Acceleration of neuronal precursors differentiation induced by substrate nanotopography. Biotechnol Bioeng 108: 2736–2746.

Mirzadeh H, Shokrolahi F, Daliri M. 2003. Effect of silicon rubber crosslink density on fibroblast cell behavior in vitro. J Biomed Mater Res A 67:727–732.

Park J, Bauer S, Von der Mark K, Schmuki P. 2007. Nanosize and vitality: TiO_2 nanotube diameter directs cell fate. Nano Lett 7:1686–1691.

Schoen I, Hu W, Klotzsch E, Vogel V. 2010. Probing cellular traction forces by micropillar arrays: Contribution of substrate warping to pillar deflection. Nano Lett 10:1823–1830.

Smith LA, Liu X, Hu J, Wang P, Ma PX. 2009a. Enhancing osteogenic differentiation of mouse embryonic stem cells by nanofibers. Tissue Eng Part A 15:1855–1864.

Smith LA, Liu X, Hu J, Wang P, Ma PX. 2009b. Enhancing osteogenic differentiation of mouse embryonic stem cells by nanofibers. Tissue Eng Part A 15:1855–1864.

Soen Y, Mori A, Palmer TD, Brown PO. 2006. Exploring the regulation of human neural precursor cell differentiation using arrays of signaling microenvironments. Mol Syst Biol 2:37.

Sun M, Graham JS, Hegedüs B, Marga F, Zhang Y, Forgacs G, Grandbois M. 2005. Multiple membrane tethers probed by atomic force microscopy. Biophys. J 89:4320–4329.

Taylor AM, Rhee SW, Tu CH, Cribbs DH, Cotman CW, Jeon NL. 2003. Microfluidic multicompartment device for neuroscience research. Langmuir 19:1551–1556.

Tee S-Y, Fu J, Chen CS, Janmey PA. 2011. Cell shape and substrate rigidity both regulate cell stiffness. Biophys J 100:L25–L27.

Thomson JA, Itskovitz-Eldor J, Shapiro SS, Waknitz MA, Swiergiel JJ, Marshall VS, Jones JM. 1998. Embryonic stem cell lines derived from human blastocysts. Science 282:1145–1147.

Wang G, Ao Q, Gong K, Wang A, Zheng L, Gong Y, Zhang X. 2010. The effect of topology of chitosan biomaterials on the differentiation and proliferation of neural stem cells. Acta Biomater 6:3630–3639.

Wang P-Y, Tsai W-B, Voelcker NH. 2012. Screening of rat mesenchymal stem cell behaviour on polydimethylsiloxane stiffness gradients. Acta Biomater 8:519–530.

Weiss P, Garber B. 1952. Shape and movement of mesenchyme cells as functions of the physical structure of the medium. Proc Natl Acad Sci USA 38:264–280.

Yim EKF, Pang SW, Leong KW. 2007. Synthetic nanostructures inducing differentiation of human mesenchymal stem cells into neuronal lineage. Exp Cell Res 313:1820–1829.

Zajac AL, Discher DE. 2008. Cell differentiation through tissue elasticity-coupled, myosin-driven remodeling. Curr Opin Cell Biol 20:609–615.